

## Valence excitations in individual single-wall carbon nanotubes

Thomas Stöckli,<sup>a),b)</sup> Jean-Marc Bonard, and André Châtelain

*Institut de Physique Expérimentale, Département de Physique, Ecole Polytechnique Fédérale de Lausanne, CH-1015 Lausanne, Switzerland*

Zhong Lin Wang

*School of Materials Science and Engineering, Georgia Institute of Technology, Atlanta, Georgia 30332-0245*

Pierre Stadelmann

*Centre Interdépartemental de Microscopie Electronique, Ecole Polytechnique Fédérale de Lausanne, CH-1015 Lausanne, Switzerland*

(Received 1 November 2001; accepted for publication 13 February 2002)

We report on measurements of the plasmon losses of individual single-wall carbon nanotubes by electron energy-loss spectroscopy in a high-resolution transmission electron microscope. The experimental data are compared to simulated excitation probabilities calculated using the hydrodynamic theory of the interaction between a probe electron and a two-dimensional quasifree electron gas confined on a cylindrical shell. Depending on the nanotube geometry, the first- or the second-order oscillation mode dominates the loss spectrum. The resonance energy of the dominant resonance mode is found to depend on the radius of the nanotube. © 2002 American Institute of Physics. [DOI: 10.1063/1.1469685]

Surface plasmons are about to live through a period of revival. Longly regarded as a subject of purely academic interest—the only practical example being the red stained church glasses produced by gold clusters—they are now rediscovered in a variety of systems such as photonic band gap structures,<sup>1</sup> near transmission through holes,<sup>2</sup> or as a spectroscopic tool.<sup>3</sup> Here we report a comparison between recent theoretical developments<sup>4</sup> and electron energy loss (EEL) data of plasmon excitations of a textbook cylindrical shell system, a single-wall carbon nanotube.

Single-wall carbon nanotubes, synthesized by the arc discharge method,<sup>5</sup> were prepared for the experiments by dipping a holey carbon transmission electron microscopy (TEM) grid into a nanotube containing ethanol dispersion. The measurements were performed on a Hitachi HF 2000 field emission TEM equipped with a Gatan 666 parallel detection EEL spectrometer. Since single-wall carbon nanotubes are sensitive to electron irradiation we have operated the microscope at 100 keV (standard setting 200 keV). Radiation damages were further minimized by selecting the area of interest by the spectrometer aperture in the diffraction coupling mode.<sup>3,6</sup> A series of eight spectra was acquired on each nanotube with an acquisition time of 0.5 s per spectra. Just before spectrum acquisition, the electron beam was condensed until the zero loss in the EEL spectrum was just below saturation. This typically resulted in a peak current density of approximately 5 A/cm<sup>2</sup> during spectrum acquisition. After correction for the nonlinearity of the detector response<sup>6</sup> and for the size of the electron probe,<sup>7</sup> the plasmon excitation probability was derived from the raw spectrum by division through the number of counts under the zero-loss peak.<sup>3,8</sup>

Figure 1 shows high-resolution TEM micrographs of two

0.61 nm radius single-wall carbon nanotubes. The images (a) and (c) were taken before and (b) and (d) after the spectrum acquisition. No significant changes of the structures can be observed after the measurement.

In Fig. 2 the first (a) and the last (b) raw EEL spectrum of a time series acquired on the single-wall nanotube shown in Figs. 1(a) and 1(b) are displayed. Only a slight broadening of the signal with exposure time can be observed. This demonstrates that the data acquisition was stopped before radiation damage could invalidate the measurements. In Fig. 2(c) the zero loss peak recorded on a zone just beside the nanotube is shown. This illustrates that the signal of an individual nanotube can clearly be resolved. Figure 3 shows the plasmon excitation probability for (a) two nanotubes of 0.61 nm radius and (b) two tubes of 0.67 nm radius (tubes with radii of 0.61 and 0.67 nm were observed predominately in our

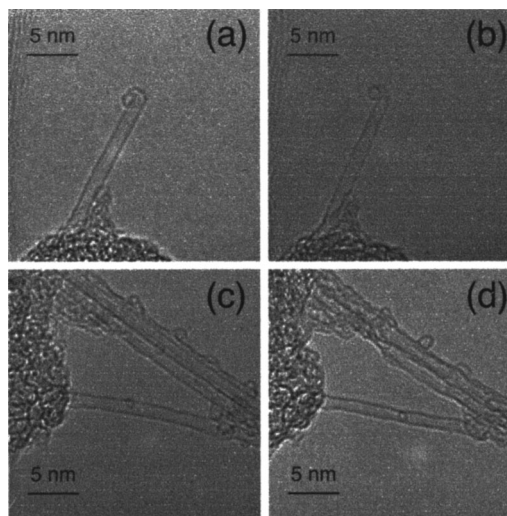


FIG. 1. High-resolution TEM micrographs of two single-wall carbon nanotubes before [(a) and (c)] and after [(b) and (d)] the spectrum acquisition.

<sup>a)</sup>Electronic mail: thomas.stoeckli@csem.ch

<sup>b)</sup>Present address: Centre Suisse d'Electronique et de Microtechnique (CSEM), Untere Gröndlistrasse 1, CH-6055 Alpnach, Switzerland.

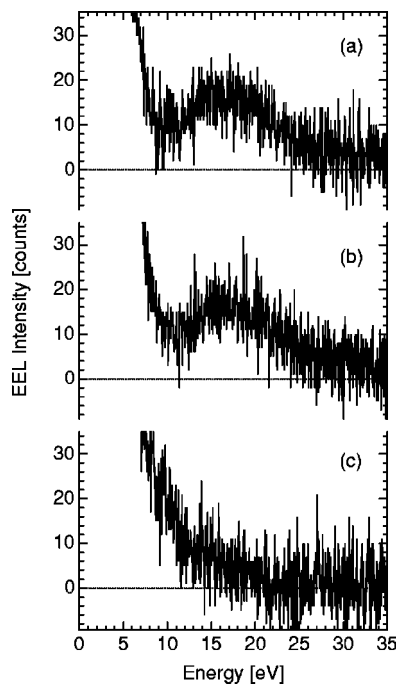


FIG. 2. Raw experimental EEL data obtained from the single-wall carbon nanotube shown in Figs. 1(a) and 1(b). The spectra labeled (a) and (b) were the first and the last, respectively, of the series of eight spectra that were acquired on each tube. (c) Zero-loss spectrum obtained beside the carbon nanotube.

samples). For better visibility a high-frequency filter has been applied to the raw data. For each radius, two behaviors can be identified. The first (solid lines) shows a maximum at lower energies than the second, traced in dashed lines. Comparing Figs. 3(a) and 3(b) it can be observed that both absorption features are shifted to lower energies in the larger nanotube.

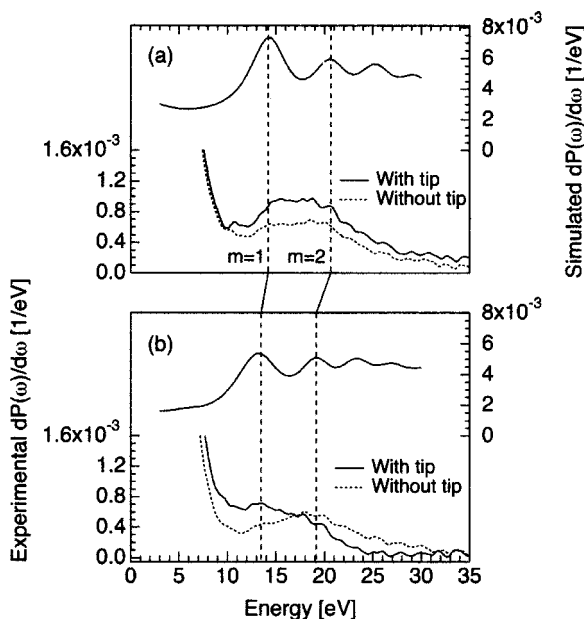


FIG. 3. (a) Measured excitation probabilities of single-wall nanotubes of 0.61 nm radius compared to simulations for a 0.6 nm radius tube. (b) Measured excitation probabilities of single-wall nanotubes of 0.67 nm radius compared to simulations for a 0.7 nm radius tube. A resonance parameter  $\omega_p$  of 27.5 eV, a damping coefficient  $\gamma$  of 5 eV, and a cutoff wavevector  $q_c$  of  $1 \text{ nm}^{-1}$  have been taken for the simulations.

To gain a qualitative understanding of the experimental data we have combined the hydrodynamic formalism of plasmon excitations by fast electrons<sup>9</sup> with the approach<sup>10–12</sup> that consists in modeling a nanotube as a gas of quasifree electrons confined onto an infinitely long cylindrical shell.<sup>4</sup> The difference between our approach and models of the plasmons of single-wall nanotubes reported earlier (see Ref. 4 and references therein) is, that our formalism yields the plasmon excitation probability for TEM electrons for the exact geometry of our experiments. The simulations, therefore, can directly be compared to the measurements reported here. The excitation probabilities have been calculated for 100 keV probe electrons. Since no angle limiting apertures were used for the spectrum acquisition the maximum scattering angle is given by the plasmon cutoff wave vector.<sup>9,13</sup> Simulations have been carried out with cutoff wave vectors of 1 and  $10 \text{ nm}^{-1}$ . The parameters for the two-dimensional electron gas are the resonance energy  $\omega_p$  of the bulk plasmon of graphite (27.5 eV), the thickness of the graphitic shell (0.34 nm), the damping coefficient (5 eV), and the Fermi velocity ( $8.110 \times 10^5 \text{ ms}^{-1}$ ).<sup>14,15</sup> In Fig. 3 the excitation probabilities calculated for a 0.6 and 0.7 nm radius nanotube are compared to the experimental data. The simulations show a series of local maxima which are due to the different plasmon resonance modes in cylindrical geometry.<sup>4</sup> We observe that for both radii the maximum of the solid lines coincides with the first order oscillation mode of the simulations, while the maximum of the dashed lines coincides with the second order oscillation mode. The energy shift of each maximum from the larger to the smaller tube is correctly reproduced by the model. An explanation why in some cases the first and in others the second order oscillation mode is more intense can qualitatively be deduced from the hydrodynamic model. In fact, the model assumes that carbon nanotubes are infinitely long.<sup>4</sup> For a tube of finite length, the wavelength of the charge density fluctuations along the tube axis cannot be longer than the tube. In consequence, the wave vector  $q$  must satisfy the additional condition  $1/l \leq q \leq q_c$ , where  $l$  is the length of the nanotube. The simulations show that higher order modes are principally excited by electrons undergoing a large wave vector transfer. If only an upper bound to the  $q$  transfer is considered, the first order oscillation is in most circumstances the most intense mode. However, if due to the finite length there is a lower limit, the excitation of the first order oscillation can be suppressed. There also is some experimental evidence that the first order mode is enhanced when the spectrum is recorded close to a nanotube tip (solid lines in Fig. 3). This means that when modeling a nanotube of finite length, care needs to be taken to select appropriate boundary conditions. A tube tip will reflect the plasmon oscillations back to the tube body. On the other hand, the plasmons will be heavily damped on the extremity that terminates into a bundle.

From Fig. 3 it can be observed that the simulations predict stronger resonances than actually measured. The experimental data are broader than the simulations since we have assumed ideal experimental conditions. However, experimental imperfections (energy distribution of the incident electrons and imperfections of the detection system) cannot account for the entire difference. An explanation could be the

approximations of the hydrodynamic theory. However, single-wall carbon nanotubes are very thin, such that quasi-elastic scattering or diffraction effects can be excluded.<sup>8</sup> Relativistic corrections increase the theoretical excitation probability<sup>16</sup> and the difference between simulated and experimental curves would become even larger. This strongly suggests that the finite length of the nanotubes probably is also responsible for the difference in intensity between theory and measurement.

The comparison of the experimental data with simulated excitation probabilities has allowed us to interpret different experimentally observed plasmon resonance behaviors of single-wall carbon nanotubes. Depending on the length and probably also the termination of the nanotube, the first or the second order cylindrical oscillation mode dominates the spectrum. This study shows that it is possible to observe higher order surface excitation modes by EELS.<sup>17</sup> The experimental data strongly support the theoretical prediction that the plasmon resonance energy depends on the radius of the nanotube. Due to the rather narrow diameter distribution of the investigated nanotubes (given by the synthesis method) it was, however, not possible to draw a very detailed picture of this size dependence. Our results can be compared to the energy loss spectra reported for the energy loss spectra reported for a nanotube bundle<sup>18</sup> or for an electron transparent nanotube film.<sup>19</sup> In both cases a broad resonance centered at 21.5 eV is observed. Our measurements show that this broad feature can be attributed to the superposition of the plasmons of many individual tubes. The fine structure of individual tubes is lost since tubes of different diameter are present in the bundle and also because the plasmons of individual tubes are coupled.

This work was partially financed by the Swiss National Science Foundation, Grant No. 2100-037660. Their support is gratefully acknowledged.

- <sup>1</sup>E. Yablonovich, Phys. Rev. Lett. **58**, 2059 (1987).
- <sup>2</sup>T. W. Ebbesen, H. J. Lezec, H. F. Ghaemi, T. Thio, and P. A. Wolff, Nature (London) **391**, 667 (1998).
- <sup>3</sup>R. F. Egerton, *Electron Energy-Loss Spectroscopy in the Electron Microscope* (Plenum, New York, 1996).
- <sup>4</sup>T. Stöckli, J.-M. Bonard, A. Châtelain, Z. L. Wang, and P. Stadelmann **64**, 115424 (2001).
- <sup>5</sup>S. Iijima and T. Ichihashi, Nature (London) **363**, 603 (1993).
- <sup>6</sup>T. Stöckli, Ph.D. thesis, Swiss Federal Institute of Technology of Lausanne, 1999.
- <sup>7</sup>At a magnification of 300 000 $\times$ , the smallest spectrometer entrance aperture (1 mm) selects a circular area of approximately 3.3 nm diameter. Assuming that the excitation probability is constant inside the tube and zero outside the tube, we have multiplied the counts by the ratio between the total area of the electron probe and the area covered by the nanotube (2.2 in our case).
- <sup>8</sup>T. Stöckli, J.-M. Bonard, A. Châtelain, Z. L. Wang, and P. Stadelmann, Phys. Rev. B **61**, 5751 (2000).
- <sup>9</sup>F. Bloch, Z. Phys. **81**, 363 (1933). For a review of more recent work, see Z. L. Wang, Micron **27**, 265 (1996).
- <sup>10</sup>C. Yannouleas, E. N. Bogachek, and U. Landman, Phys. Rev. B **50**, 7977 (1994).
- <sup>11</sup>C. Yannouleas, E. N. Bogachek, and U. Landman, Phys. Rev. B **53**, 10225 (1996).
- <sup>12</sup>X. Jiang, Phys. Rev. B **54**, 13487 (1996).
- <sup>13</sup>H. Raether, *Excitation of Plasmons and Interband Transitions by Electrons* (Springer, Berlin, 1980).
- <sup>14</sup>J. Daniels, C. Festenberg, H. Raether, and K. Zeppenfeld, *Optical Constants of Solids by Electron Spectroscopy* (Springer, Berlin, 1979).
- <sup>15</sup>P. R. Wallace, Phys. Rev. **71**, 622 (1947).
- <sup>16</sup>R. Garcia-Molina, A. Gras-Marti, A. Howie, and R. H. Ritchie, J. Phys. C **18**, 5335 (1985).
- <sup>17</sup>The quadrupolar mode of spherical particles has been observed by infrared spectroscopy on Au coated silica particles in a glass matrix: S. J. Oldenburg, J. B. Jackson, S. L. Westcott, and N. J. Halas, Appl. Phys. Lett. **75**, 2897 (1999).
- <sup>18</sup>R. Kuzuo, M. Terauchi, and M. Tanaka, Jpn. J. Appl. Phys., Part 2 **33**, L1316 (1994).
- <sup>19</sup>T. Pichler, M. Knupfer, M. S. Golden, J. Fink, A. G. Rinzler, and R. E. Smalley, Phys. Rev. Lett. **80**, 4729 (1998).